Experimental Neurology 236 (2012) 179–189

Contents lists available at SciVerse ScienceDirect

Experimental Neurology

journal homepage: www.elsevier.com/locate/yexnr

Tail spasms in rat spinal cord injury: Changes in interneuronal connectivity

Sandra Kapitza [a,1], Björn Zörner [a,*,1], Oliver Weinmann [a], Marc Bolliger [b], Linard Filli [a], Volker Dietz [b], Martin E. Schwab [a]

[a] Brain Research Institute, University and ETH Zurich, Winterthurerstrasse 190, 8057 Zurich, Switzerland
[b] Spinal Cord Injury Center, Balgrist University Hospital, Forchstrasse 340, 8008 Zurich, Switzerland

ARTICLE INFO

Article history:
Received 22 January 2012
Revised 16 April 2012
Accepted 23 April 2012
Available online 1 May 2012

Keywords:
Spasticity
Spinal cord injury
Spinal networks
Interneuron
Immunohistochemistry

ABSTRACT

Uncontrolled muscle spasms often develop after spinal cord injury. Structural and functional maladaptive changes in spinal neuronal circuits below the lesion site were postulated as an underlying mechanism but remain to be demonstrated in detail. To further explore the background of such secondary phenomena, rats received a complete sacral spinal cord transection at S_2 spinal level. Animals progressively developed signs of tail spasms starting 1 week after injury. Immunohistochemistry was performed on $S_{3/4}$ spinal cord sections from intact rats and animals were sacrificed 1, 4 and 12 weeks after injury.

We found a progressive decrease of cholinergic input onto motoneuron somata starting 1 week *post*-lesion succeeded by shrinkage of the cholinergic interneuron cell bodies located around the central canal. The number of inhibitory GABAergic boutons in close contact with Ia afferent fibers was greatly reduced at 1 week after injury, potentially leading to a loss of inhibitory control of the Ia stretch reflex pathways. In addition, a gradual loss and shrinkage of GAD65 positive GABAergic cell bodies was detected in the medial portion of the spinal cord gray matter. These results show that major structural changes occur in the connectivity of the sacral spinal cord interneuronal circuits below the level of transection. They may contribute in an important way to the development of spastic symptoms after spinal cord injury, while reduced cholinergic input on motoneurons is assumed to result in the rapid exhaustion of the central drive required for the performance of locomotor movements in animals and humans.

Introduction

Muscle cramps and uncontrolled, rhythmic, clonic muscle spasms are frequent complications that develop in the first few months after a spinal cord injury (SCI) (Maynard et al., 1990). These cramps can severely affect the quality of life of paraplegic patients (Adams and Hicks, 2005). Although the underlying mechanisms are poorly understood at present, it is widely accepted that the pathogenesis of spastic symptoms is multifactorial (Dietz and Sinkjaer, 2007; Nielsen et al., 2007). Hence, the appearance of muscle spasms cannot be exclusively explained by the loss of inhibitory supraspinal projections since spastic symptoms appear gradually with a delay of several weeks or months after injury suggesting the presence of additional, rather slowly and secondarily developing processes of adaptation. Results from electrophysiological studies conducted over the last 40 years in humans with brain or spinal cord injury indicate that spontaneous secondary maladaptive changes, such as inefficient inhibition of local reflex pathways, occur in spinal circuits distal to the lesion (Delwaide and Penders, 1969; Dietz, 2010; Faist et al., 1994; Kitzman, 2006; Little and Halar, 1985; Mailis and Ashby, 1990). Activation of motoneurons, e.g., via excitatory Ia afferents from muscle spindles, is regulated by presynaptic inhibition from GABAergic interneurons, autogenic inhibition from Golgi tendon organs, disynaptic reciprocal inhibition from muscle spindles of antagonistic muscles and recurrent inhibition via Renshaw cells (Nielsen et al., 2007). Following injury, a progressive decline of these control mechanisms could result in reduced spinal inhibition (disinhibition) and, therefore, unrestrained reflex transmission. In addition, altered intrinsic properties of motoneurons, e.g., increased excitability due to changed receptor expression profiles, have been linked to the development of spastic symptoms (Khristy et al., 2009; Li et al., 2004; Murray et al., 2010a, 2010b; Ryge et al., 2010; Wienecke et al., 2010). Changes in gene expression can lead to the spontaneous reappearance of prolonged motoneuronal depolarizations (plateau potentials) as observed after SCI in animal models (Bennett et al., 2001; Gorassini et al., 2004; Li et al., 2004).

Information about the possible pathophysiological roles of axonal or dendritic sprouting or pruning and circuit reorganization below the injury site and their contribution to the development of spastic symptoms and signs is sparse. After damage to the central nervous system (CNS), neuronal networks can spontaneously reorganize via the formation of new connections and fiber sprouting, generally referred to as structural plasticity. Recent animal studies have

* Corresponding author at: Department of Neurology, University Hospital Zurich, Frauenklinikstr. 26, 8091 Zurich, Switzerland. Fax: +41 44 255 43 80.
E-mail address: bjoern.zoerner@usz.ch (B. Zörner).
[1] Both authors contributed equally to the study.

0014-4886/$ – see front matter © 2012 Elsevier Inc. All rights reserved.
doi:10.1016/j.expneurol.2012.04.023

demonstrated that structural plasticity can mediate functional recovery after CNS injury (Courtine et al., 2008; Raineteau and Schwab, 2001; Schwab, 2010; Zorner and Schwab, 2010). Nevertheless, inappropriate sprouting, pruning or rewiring of connections might also lead to an imbalance in neuronal networks and malfunctions such as chronic pain, spasms or autonomic dysfunction (Krassioukov and Weaver, 1996; Llewellyn-Smith and Weaver, 2001; Llewellyn-Smith et al., 2006; Weaver et al., 1997). Classical electrophysiological and anatomical studies performed more than 50 years ago in monkeys and cats with spinal cord hemisections suggested that sprouting of primary afferent fibers occurred below the lesion site, thus leading to an excitatory overbalance and spastic signs (McCouch et al., 1958). However, more recent studies either failed to show sprouting of primary afferents (Nacimiento et al., 1993, 1995a, 1995b) or failed to directly link the sprouting response with the emergence of secondary malfunctions (Helgren and Goldberger, 1993; Krenz and Weaver, 1998; Murray and Goldberger, 1974).

In a series of studies, Kitzman investigated structural changes below a traumatic SCI focusing on the morphology of motoneurons and their synaptic input (Kitzman, 2005, 2006, 2007). Kitzman used the rat spastic tail model based on a complete spinal S_2 lesion (Bennett et al., 1999). This model shows major sequels of a spinal cord transection, in particular pronounced hyperreflexia, muscle spasms after gentle touch and the reappearance of plateau potentials in motoneurons (Bennett et al., 1999, 2001, 2004). In lesioned rats, a progressive decrease in the number of dendritic branches per motoneuron and a shift of the synaptic input on motoneuron somata and proximal dendrites towards excitation was found (Kitzman, 2005, 2006). Both findings were temporally associated with the gradual appearance of spastic signs/spasms. However, changes at interneuronal levels were not investigated. The objective of the present study was to analyze structural changes in spinal neuronal networks below the lesion site in the rat spastic tail model focusing on relevant types of interneurons and their connections.

Material and methods

Animals

18 adult female Lewis rats (200–270 g, Centre d'Elevage R. Janvier) received a complete sacral SCI and were randomly assigned to one of three different survival groups (1 week, 4 weeks or 12 weeks survival after SCI) with 5–7 animals in each group. 12 rats of the same age and weight without SCI served as controls (intact) for immunohistochemistry. Rats were housed in groups of 3–5 animals per cage in a 12:12 h light:dark cycle. Food and water were supplied ad libitum. All experimental procedures were performed with the approval of the Veterinarian Office Zurich, Switzerland.

Spinal cord injury

Complete sacral spinal cord transections were performed as described previously (Bennett et al., 1999, 2004). In brief, rats were deeply anesthetized with subcutaneous injections of Hypnorm and Dormicum (Hypnorm, 120 µl per 200 g body weight, Janssen Pharmaceutics; Dormicum, 0.75 mg per 200 g body weight, Roche Pharmaceuticals). The L_2 vertebra was identified using the prominent dorsal process L_5 as a reference. Deep back muscles overlying L_2 were removed followed by a partial laminectomy of the L_2 vertebra. The dura was opened longitudinally with a sharp needle and 200 µl lidocaine (1%) was applied topically to prevent movements of the hind limbs during spinal root manipulations. The lumbar roots were carefully pushed aside with a small sponge to gain access to the sacral spinal cord (Fig. 1A, B). In Lewis rats, the entrance zone of the small S_2 dorsal roots, i.e., the S_2 spinal segment was located at the very rostral end of the L_2 vertebra. Complete transection of the sacral spinal cord at S_2 spinal level was performed with sharp iridectomy scissors under a surgical microscope. During transection, care was taken to preserve the ventral and dorsal blood vessels in order to maintain blood circulation in the sacral spinal cord and to avoid spinal infarction potentially leading to the "dead tail syndrome" (Bennett et al., 1999). Intact control animals were "sham operated", i.e., animals received a laminectomy and dura opening but no spinal cord transection. Subsequently, back muscles were sutured and the skin was closed with surgery staples. *Post*-operative care included daily subcutaneous injections of antibiotics (Baytril, 5 mg per kg body weight, Bayer AG) and analgesics (Rimadyl, 2.5 mg per kg body weight, Pfizer AG) over a period of at least 1 week. The rats' well-being was checked daily for the entire duration of the experiment.

Behavioral assessment of spasticity

Rats were evaluated in their home cages for signs of tail spasticity before surgery (baseline) and at weeks 1, 2, 3, 4, 6, 8 and 12 after SCI. Responses to pinching of the tip of the tail using thumb and index finger were scored on a scale from 0 to 4 according to the developmental stages of tail spasticity determined by Bennett et al. (1999). Briefly, 0 described an active retraction of the tail in response to pinching as seen in intact animals, 1 was characterized by tail flaccidity and hypotonus, but also a slight bending of the tip of the tail in response to pinching indicating that the severed sacral spinal cord was alive, 2 described slight and short-lasting flexor muscle hypertonus with ventral coiling, some flicking and mild clonus, 3 was similar to 2 but stronger in amplitude demonstrating apparent coiling and long-lasting spasms after pinching, and 4 was characterized by the presence of strong hypertonus in flexor and extensor muscles, massive clonus, coiling and spasms as well as a whiplash-like movement in response to pinching and an S-shaped tail during walking. Only animals that showed at least a slight tail reaction in response to pinching 1 week after SCI were included in the study to assure viability of the sacral spinal cord after lesion. Assessment of tail spasticity was performed by the same person throughout the experiment.

Electrophysiological assessment of muscle spasms and H-reflex

The testing procedure was adopted from Bennett et al. (2004). Before surgery, rats that survived 12 weeks after SCI were trained to sit in a Plexiglas tube with their tail hanging freely out of the tube. The same rats were tested before surgery (baseline) and 1, 2, 3, 4, 6, 8 and 12 weeks after SCI. Two slings made of steel wire served as stimulation electrodes and were, at first, fixed to the tip of the tail for stimulation of cutaneous afferents in order to elicit muscle spasms and, second, close to the base of the tail to stimulate Ia afferents for H-reflex measurements. H-reflexes were not determined in intact rats since electrical stimulation at the base of the tail can induce discomfort in addition to active tail movements that interfere with the reflex measurements. Electromyographic recordings (EMGs) from short segmental tail muscles were performed using self-made steel needle electrodes. As a reference point the Ca_{12} tail vertebra was defined which corresponds approximately to the midpoint of the tail. EMG electrodes were attached 1 and 2.5 cm above this reference point while stimulation electrodes were placed 2.5 and 4.5 cm below this landmark. The recording ground was placed 1 cm below the reference point. To ensure consistent placement of the electrodes throughout the experiment, the animals' tails were marked with a waterproof pen at the described locations. At the beginning of each testing session, motor thresholds were determined by gradually increasing the stimulus intensity until a first subtle tail movement was observed. For assessment of muscle spasms, EMG responses of segmental tail muscles were recorded after electrical stimulation (train at 100 Hz for 0.5 s, pulse width 0.2 ms) of cutaneous afferents at the tip of the tail at different time points after injury. To elicit an H-reflex response,

electric stimuli were applied at 1.5× motor threshold with a 0.2 ms pulse delivered at 2–20 s intervals. A monosynaptic H-reflex, i.e., short latency reflex, was defined as an early response with latencies from 10–15 ms after stimulus onset. Muscle signals were digitized (PowerLab 8/30, ADInstruments, Oxford, UK) with a sampling rate of 10 kHz, amplified (gain of 2500), and high- and low-pass filtered (100–5000 Hz). The response was quantified by integrating the rectified EMG signal within the time window defined for early, monosynaptic responses (10–15 ms). Values obtained from multiple trials were averaged per session. Then, H-reflex responses observed 1 week after injury were averaged for all animals and results measured at a given time point after lesion for each separate animal were normalized to this mean value. Data were recorded using the commercially available software LabChart v6.1.1 (ADInstruments, Oxford, UK).

Perfusion and tissue preparation

Rats were deeply anesthetized with an intraperitoneal injection of pentobarbital (1.25 ml/kg, Eutha® 77, Provet) and perfused transcardially with 100 ml heparinized Ringer solution followed by 500 ml phosphate-buffered fixative solution with 4% paraformaldehyde (PFA), 0.05% glutaraldehyde, 5% sucrose and 70 mg/l $CaCl_2$ (pH 7.4). After dissection, sacral spinal cords were *post*-fixed for 12 h in glutaraldehyde-free fixative solution at 4 °C. Subsequently, spinal cords were soaked for 3 days in phosphate-buffered sucrose (25%) to cryoprotect the tissue. The dura was removed and spinal cords were embedded in Tissue-Tek O.C.T. and frozen in isopentane at −40 °C. Spinal cords were cut on a cryostat and 40 μm thick cross-sections were collected either on-slide (for Cresyl violet staining) or free floating (for immunohistochemistry). On-slide sections were dried overnight whereas free floating sections were stored at −20 °C in an antifreeze solution containing 15% glucose and 30% ethylenglycol in phosphate-buffered saline (50 mM).

Nissl staining and immunohistochemistry (IHC)

Nissl staining was used to confirm that spinal cord lesions were complete (Fig. 1C–E). Cross-sections of the lesion site were collected on-slide and dried overnight. All sections were bathed in Cresyl violet solution for 3 min, dehydrated in ethanol and washed in xylol before they were coverslipped with Eukitt. Immunohistochemical stains were performed on cross-sections from spinal cord sacral segments S_3 and S_4 with commercially available antibodies. Primary and secondary antibody specifications and dilutions used in this study are listed in Table 1.

For detection of boutons on motoneuron somata which were positive for vesicular glutamate transporter 2 (vGLUT2) and vesicular acetylcholine transporter (vAChT; C-boutons), sections were *post*-fixed for 20 min at room temperature (RT) in a phosphate-buffered solution containing 4% PFA, 0.05% glutaraldehyde and 15% picric acid. Slides were then successively treated with ammonium chloride (50 mM) in 0.1 M phosphate buffer (PB) for 30 min, with sodiumborhydrate (1%) in 0.1 M PB for 30 min and with glycine (50 mM) in 0.1 M Tris for 30 min each at RT to uncover antigens and reduce background fluorescence. Afterwards slides were washed for 30 min in a blocking solution (0.1 M PB with 4% normal goat serum and 0.3% Triton X-100) at RT followed by overnight incubation at 4 °C with the primary antibodies diluted in 0.1 M PB and containing 4% normal goat serum and 0.05% Triton X-100. The staining procedure for the vesicular GABA transporter (vGAT) included treatment with 4% phosphate-buffered PFA and 0.2% picric acid for 10 min, 50 mM ammonium chloride for 30 min and citrate buffer (pH 6.0) for 30 min. Subsequently slides were heated 3 times in a microwave for 10 s at 600 W and bathed for 30 min in 0.1 M PB blocking solution containing 4% normal goat serum and 0.05% Triton X-100. This was followed by overnight incubation at 4 °C with the primary antibodies diluted in the same blocking solution. For staining of boutons positive for glutamic acid decarboxylase 65 (GAD65, P-boutons) and boutons positive for vesicular glutamate transporter 1 (vGLUT1), sections were treated with 20% methanol for 30 min, 50 mM glycine in 0.1 M Tris for 30 min (10 min at 80 °C) and 4% normal goat serum in 0.1 M PB containing 0.3% Triton X-100 for 30 min. Sections were incubated overnight at 4 °C with the primary antibodies diluted in 0.1 M PB containing 4% normal goat serum and 0.05% Triton X-100. GAD65 immunoreactivity in spinal interneurons was detected with the same protocol except hypotonic 0.01 M PB dilution was used instead of 0.1 M Tris or PB without Triton X-100. For detection of

Table 1
Antibodies and dilutions.

Antigen detection	Primary antibody	Secondary antibody	Biotin detection
vGLUT2-positive terminals on motoneuron somata	Rabbit anti vGLUT2 (Synaptic Systems, Göttingen, Germany, 1:1000) Mouse anti NeuN (Millipore, 1:500)	Cy2 anti rabbit (Jackson ImmunoResearch, 1:100) Cy3 anti mouse (Jackson ImmunoResearch, 1:300)	
vGAT-positive terminals on motoneuron somata	Rabbit anti vGAT (Synaptic Systems Göttingen Germany, 1:1000) Mouse anti NeuN (Millipore, 1:500)	Anti-rabbit biotinylated (Jackson ImmunoResearch, 1:500) Cy3 anti mouse (Jackson ImmunoResearch, 1:300)	DyLight 488 (Jackson ImmunoResearch, 1:500)
vAChT-positive terminals on motoneuron somata	Guinea pig anti vAChT (Millipore, 1:300) Mouse anti NeuN (Millipore, 1:500)	Anti-Guinea pig biotinylated (Jackson ImmunoResearch, 1:500) Cy3 anti mouse (Jackson ImmunoResearch, 1:300)	DyLight 488 (Jackson ImmunoResearch, 1:500)
GAD65-positive terminals (P-Boutons) around vGLUT1-containing axon terminals in lamina IX	Rabbit anti GAD65 (Sigma, 1:250) Mouse anti vGLUT1 (Synaptic Systems, Göttingen, Germany, 1:200)	Anti-rabbit biotinylated (Jackson ImmunoResearch, 1:500) Cy3 anti mouse (Jackson ImmunoResearch, 1:300) Nissl Cy5 (Invitrogen, Molecular Probes, 1:500)	DyLight 488 (Jackson ImmunoResearch, 1:500)
GAD65-immunoreactive neurons in lamina VII	Rabbit anti GAD65 (Sigma, 1:250) Mouse anti NeuN (Millipore, 1:500)	Cy2 anti rabbit (Jackson ImmunoResearch, 1:200) Cy5 anti mouse (Jackson ImmunoResearch, 1:500)	
ChAT-immunoreactive neurons in lamina VII	Goat anti ChAT (Millipore, 1:250) Mouse anti NeuN (Millipore, 1:500)	Donkey anti goat Alexa 488 (Jackson ImmunoResearch, 1:500) Cy3 anti mouse (Jackson ImmunoResearch, 1:300)	

choline acetyltransferase (ChAT) in the cytoplasm of interneurons, sections were carefully permeabilized for 2 h with hypotonic 0.01 M PB containing 0.3% Triton X-100 followed by overnight incubation with the primary antibodies diluted in TNB buffer (0.1% casein, 0.25% bovine serum albumin, purified bovine gelatin proteins (25% Top block, LuBioScience GmbH, Luzern, Switzerland), 0.15 M NaCl, 0.05% Tween in 0.1 M Tris buffer). After incubation with the primary antibodies all sections were washed 3 times in phosphate-buffered saline (0.1 M) and incubated for 1 h at RT in TNB blocking solution containing the secondary antibodies. For staining of vAChT, vGAT and P-boutons sensitivity was increased by using the biotin/streptavidin system. Following incubation with biotinylated antibodies, sections were washed 3 times and incubated for 1 h at RT with fluorescent streptavidin conjugates. Finally sections were mounted on glass-slides, dried for 36 h at 4 °C and coverslipped with Mowiol.

Quantification of immunoreactivity

Micrographs were taken with a Leica TCS SP2 confocal microscope using a 63× oil immersion objective (HCX PL APO oil, 1.32 numerical aperture) and Arg/ArgKr 488 nm, GreNe 543 nm and HeNe 633 nm lasers. The pinhole was set at 1.49 Airy units. Photomultiplier- (PMT) gain and offset were adjusted to mean levels and kept constant for all micrographs. Pixel size was 0.12 μm with 1024×1024 pixels per image. For each analysis and staining a Z-axis image stack (stack depth 8–12 μm, Z step-size 0.6 μm) was acquired on an extra section and immunoreactivity was quantified with ImageJ software. The optimal antibody penetration depth was defined by the highest intensity of the immunoreactive signal. For each staining series the predefined Z-axis for each antigen was reassessed and slight adjustments were made (±2 μm). Double and triple immunofluorescence images were generated and converted to Photoshop files (Adobe Photoshop CS3 Extended, Adobe). Brightness of the images was adjusted to improve signal-to-noise ratio. To examine the number of axosomatic boutons per motoneuron, images were taken randomly from the ventral region of the sacral spinal cord. Criteria for a cell (counterstained with NeuN, for antibodies, see Table 1) to be considered as motoneuron and being subjected to further analysis were the presence of a cell body in Rexed's lamina IX, a cell body diameter larger than 40 μm, a clear outline of the cell body and a visible nucleus (adapted from Kitzman, 2006). Perimeter of motoneurons was measured with the ImageJ software (National Institutes of Health). vGLUT-2 (glutamatergic synapses; Oliveira et al., 2003; Todd et al., 2003), vGAT (GABAergic and glycinergic synapses; Chaudhry et al., 1998; McIntire et al., 1997; Todd and Sullivan, 1990) and vAChT (cholinergic synapses; Arvidsson et al., 1997; Gilmor et al., 1996; Usdin et al., 1995) immunoreactive boutons in close contact with the cell membrane of motoneurons were counted manually. Criteria for a bouton to be analyzed were proximity to the motoneuron cell membrane, clear discrimination between adjacent boutons and optimal antibody penetration depth. 175–308 motoneurons were analyzed per animal group and staining. The number of boutons was averaged for each animal and group and reported as number per 100 μm (motoneuron) cell membrane. Excitatory Ia afferent fibers convey sensory information from muscle spindles to motoneurons (monosynaptic stretch reflex) and their terminals are positive for vGLUT1 (Alvarez et al., 2004; Landry et al., 2004; Oliveira et al., 2003; Todd et al., 2003). This reflex pathway is controlled by inhibitory GABAergic GAD65 positive terminals, so called P-boutons (Betley et al., 2009; Hughes et al., 2005). GAD65 positive boutons were counted as P-boutons only if fluorescent labeling suggested contact between the GAD65 positive boutons and the vGLUT1 positive afferent fiber which had a diameter of at least 2 μm. In total, 4018 vGLUT1 positive afferent fibers were analyzed in Rexed's lamina IX. Numbers per field were averaged for each animal and group. The number and size of spinal neurons either immunopositive for ChAT or GAD65, resembling cholinergic and GABAergic interneurons, respectively, were analyzed in Rexed's lamina VII. For each marker, two images (0.37 μm per pixel, 1024×1024 pixels) were captured from two adjacent areas close to the central canal using a 40× oil immersion objective (HCX PL APO oil, 1.25 numerical aperture). Each image was analyzed regarding the number and size, i.e., the area, of the immunoreactive cell bodies using ImageJ. Cell numbers were given per 10 μm section thickness (ChAT) or per field (GAD65) and cell body sizes were averaged for each marker and animal group.

For densitometric quantification of vGAT, GAD65, vGLUT1 and vGLUT2 immunoreactivity in Rexed's laminae I–III and VII, images were captured with a cooled CCD Camera (CoolSNAP, Roper Scientific, Ottobrunn, Germany) and digitized with MCID Elite 7.0 Imaging System (Imaging Research, Ontario, Canada). The same exposure time was used for all images of a particular staining. Images were taken from the medial and lateral portion of Rexed's lamina VII and the dorsal horn (Rexed's laminae I–III) of the sacral spinal cord. Values were normalized to background and averaged for each marker and animal group.

Statistics

Statistical analysis was performed with the SPSS software package for Windows (version 14.0; SPSS) and GraphPad Prism 5 for Windows (version 5.01; GraphPad Software). For all tests, the level of statistical significance was set a priori at $P<0.05$ indicated by an asterisk in the figures. The absence of an asterisk indicates no significant difference. Exact *P*-values for analyses of variance are given in the text (see Results section). Data are reported as

Table 2
Densitometric quantification of vGAT, GAD65, vGLUT1 and vGLUT2 immunoreactivity in medial and lateral lamina VII and in laminae I–III at spinal level S_3–S_4.

Lamina	Antigen	Group	1 week	4 weeks	12 weeks
VII medial	vGAT	Intact	1.00 ± 0.07	1.00 ± 0.07	1.00 ± 0.16
		SCI	1.17 ± 0.23	1.07 ± 0.18	1.39 ± 0.17
		P	0.5219	0.7245	0.1468
	vGLUT2	Intact	1.00 ± 0.07	1.00 ± 0.17	1.00 ± 0.09
		SCI	0.41 ± 0.14	0.76 ± 0.16	0.52 ± 0.08
		P	0.0167	0.3271	0.0072
	vGLUT1	Intact	1.00 ± 0.10	1.00 ± 0.10	1.00 ± 0.07
		SCI	0.80 ± 0.05	0.71 ± 0.09	0.51 ± 0.12
		P	0.1285	0.0771	0.0178
	GAD65	Intact	1.00 ± 0.03	1.00 ± 0.03	1.00 ± 0.07
		SCI	0.92 ± 0.09	1.06 ± 0.06	0.46 ± 0.03
		P	0.4307	0.4233	0.0015
VII lateral	vGAT	Intact	1.00 ± 0.08	1.00 ± 0.08	1.00 ± 0.16
		SCI	1.15 ± 0.26	0.92 ± 0.13	1.58 ± 0.18
		P	0.5982	0.6496	0.0556
	vGLUT2	Intact	1.00 ± 0.07	1.00 ± 0.14	1.00 ± 0.06
		SCI	0.47 ± 0.18	0.83 ± 0.10	0.89 ± 0.06
		P	0.0539	0.3771	0.2583
	vGLUT1	Intact	1.00 ± 0.11	1.00 ± 0.11	1.00 ± 0.25
		SCI	0.69 ± 0.06	0.59 ± 0.08	0.88 ± 0.18
		P	0.0657	0.0306	0.7071
	GAD65	Intact	1.00 ± 0.12	1.00 ± 0.12	1.00 ± 0.17
		SCI	0.96 ± 0.14	1.18 ± 0.09	0.91 ± 0.10
		P	0.8524	0.2531	0.6566
I–III	vGAT	Intact	1.00 ± 0.09	1.00 ± 0.09	1.00 ± 0.08
		SCI	1.02 ± 0.13	0.90 ± 0.09	1.52 ± 0.16
		P	0.9018	0.4496	0.0411
	vGLUT2	Intact	1.00 ± 0.03	1.00 ± 0.06	1.00 ± 0.08
		SCI	0.51 ± 0.18	0.94 ± 0.12	0.81 ± 0.06
		P	0.0701	0.7074	0.1075
	vGLUT1	Intact	1.00 ± 0.06	1.00 ± 0.06	1.00 ± 0.06
		SCI	0.89 ± 0.05	0.78 ± 0.08	0.77 ± 0.18
		P	0.2179	0.0805	0.2849
	GAD65	Intact	1.00 ± 0.04	1.00 ± 0.04	1.00 ± 0.07
		SCI	1.06 ± 0.12	1.27 ± 0.11	0.73 ± 0.04
		P	0.6620	0.0818	0.0172

group mean values ± S.E.M. except for the spasticity scores which are shown as group mean values ± S.D. For behavioral data analysis (spasticity scores), non-parametric two-way analysis of variance by ranks (Friedman test) was used. For standardization, H-reflex amplitudes measured 1–12 weeks after injury were normalized to the mean response amplitude measured 1 week *post*-injury and ratios were averaged for each time point. One-way ANOVA for repeated measurements was applied to detect a significant change of the H-reflex response over time. If significant, the ANOVA was followed by *post-hoc* Bonferroni's Multiple Comparison Tests comparing the ratios obtained at weeks 2, 3, 4, 6, 8 and 12 after injury with the results from 1 week after injury. For statistical analyses of immunoreactive boutons in lamina IX as well as for the analyses of the number and size of interneurons in lamina VII, one-way ANOVA was used. In case of significant results, *post-hoc* Bonferroni's Multiple Comparison Tests were performed comparing rats sacrificed 1, 4 and 12 weeks after injury with intact animals. For analysis of the densitometric quantifications in the different laminae, each SCI animal group was compared to its own separate control group of intact rats for which slices were stained simultaneously in the same procedure (3 separate intact control groups). Densitometric values measured in each animal were normalized to the mean value of the corresponding control group. Normalized values (ratios) were then averaged for each animal group, i.e., for each SCI and each control group. Student's unpaired *t*-test was applied to detect significant differences between the particular SCI animal group and the respective control group. *P*-values obtained from the *t*-tests were used to detect general pattern changes and, therefore, Bonferroni adjustments were omitted (see Table 2).

Results

After complete sacral S_2-SCI, rats progressively developed signs of tail spasticity starting with mild coiling in response to pinching 1 week after injury (Fig. 1F). During the following weeks, animals increasingly demonstrated aberrant and exaggerated tail movements after gentle manual stimulation such as extensive ventral flexion of the tail and long-lasting spastic cramps. These pathological changes were reflected by a significantly increased spasticity score ($P = 0.004$ for animals that survived 4 weeks after injury, $P < 0.0001$ for animals that survived 12 weeks after injury, Friedman test). Between 6 and 8 weeks *post*-injury, most of the animals reached the maximal spasticity score of 4 and showed a persistent S-shaped deformation of their tails. During the entire observation period, there was no evidence for impaired hind limb function or bladder and bowel dysfunction after sacral SCI. Electrical stimulations of cutaneous afferents at the tip of the tail elicited similar involuntary tail movements as observed for manual pinching. Before lesion and up to 3 weeks after injury, EMGs recorded from segmental tail muscles showed only short-lasting muscle activity (<1 s) following electrical stimulation at the tip of the tail (Fig. 1G). Starting 1 month after SCI, the duration of EMG signals increased considerably (>5 s) indicating long-lasting muscle activity in response to stimulation. The amplitude of monosynaptic H-reflexes measured 6 and 8 weeks after SCI was significantly increased in comparison to responses obtained 1 week *post*-injury ($P = 0.0014$, one-way repeated-measures ANOVA; Fig. 1H). All of these behavioral and electrophysiological data illustrate the gradual development of spastic symptoms in our rats with complete sacral SCI.

The loss of descending tracts below the lesion was reflected by a 10–50% decrease of the glutamatergic markers vGLUT1 (marker for primary afferent Ia fibers as well as corticospinal tract terminals; (Giuffrida and Rustioni, 1989)) and vGLUT2 (marker for excitatory bulbospinal tract terminals and propriospinal interneurons) in the analyzed laminae VII and I–III of spinal segments S_3–S_4 1 week *post*-injury (Table 2). In contrast, the marker for GABAergic neurons GAD65 and vGAT, present in GABAergic and glycinergic boutons, did not change substantially 1 week after spinal cord transection (Table 2). 12 weeks after lesion, we found a significant reduction of GAD65 positive boutons in the medial portion of Rexed's lamina VII, whereas vGAT showed a trend towards increased immunoreactivity in all analyzed layers at this time point (Table 2). However, there were variations in time course (decline or partial restoration) and localization (medial vs. lateral lamina VII and laminae I–III) of the different markers, which made a more detailed interpretation of the results difficult.

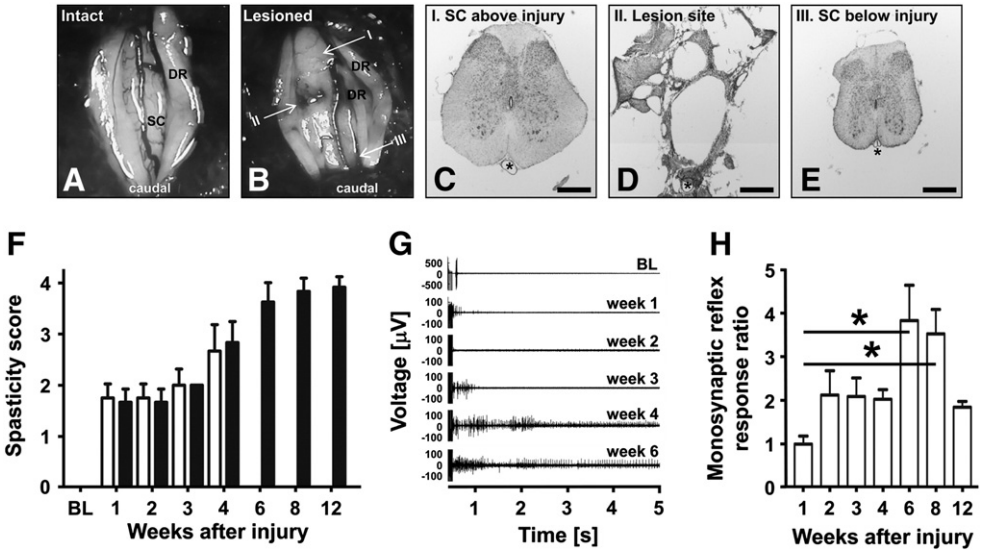

Fig. 1. Rats develop signs of spasticity in tail muscles after complete transection of the spinal cord at level S_2. Photograph of surgery site before (A) and after a complete spinal cord injury at S_2 (B). Representative Cresylviolet staining of transverse spinal cord sections above (spinal level S_1, C), at (spinal level S_2, D), and below (spinal level S_4, E) the injury site, approximately at locations illustrated in B. The center of the lesion is characterized by a complete loss of nervous tissue, scarring and cavitations while the spinal cord above and below the injury appears histologically intact. Asterisks indicate the spared anterior spinal artery. (C–E) Scale bars: 500 µm. (F) Spasticity scores at different time points before and after SCI for animals that survived for 4 weeks after lesion (white bars) and animals that survived for 12 weeks after lesion (black bars). Data are presented as animal group means ± S.D. with n = 6 animals per group and time point. (G) EMG responses of segmental tail muscles of one representative animal after electrical stimulation of cutaneous afferents at different time points after injury. (H) Development of normalized monosynaptic reflex amplitudes (H-reflex) following SCI. Data are presented as animal group means ± S.E.M., n = 6 animals per time point. DR, dorsal root; SC, spinal cord; BL, baseline. *$P < 0.05$.

We analyzed the excitatory and inhibitory synaptic input on motoneuron somata in intact rats and 1, 4 and 12 weeks after injury. In intact rats, excitatory vGLUT2 positive and inhibitory vGAT positive boutons were abundantly present in all laminae of the sacral spinal cord. One week after SCI, the number of vGLUT2 positive boutons was significantly decreased by approximately 20% and remained at that level up to 12 weeks after injury ($P=0.0028$, one-way ANOVA; Fig. 2). The number of vGAT positive boutons remained unchanged after lesion ($P=0.5075$, one-way ANOVA; Fig. 2). Consequently, the ratio of excitatory vGLUT2 to inhibitory vGAT immunoreactive boutons decreased from 0.84 in intact animals to 0.72 in rats sacrificed 12 weeks after transection (data not shown) suggesting a subtle increase of the inhibitory over the excitatory drive on motoneuron somata. Cholinergic boutons, the so-called C-boutons, represent another important excitatory input to spinal motoneurons, especially to their somata. They formed large varicosities covering up to 5 μm of the motoneuronal cell membrane. The number of C-boutons was significantly reduced in S_3–S_4 by more than 50% at 1 week and by more than 75% at 12 weeks after injury ($P<0.0001$, one-way ANOVA; Fig. 2).

A key element of spinal sensory-motor control of muscle activity is represented by the Ia fiber input from muscle spindles and its mono-, di- and polysynaptic reflex pathways. The vesicular glutamate transporter vGLUT1 is a marker of Ia afferents. Inhibitory GAD65 positive P-boutons end on these presynaptic Ia fibers, mediating presynaptic inhibition. As described previously (Hughes et al., 2005), we found that vGLUT1 positive afferents were often, i.e., in more than 40% of the cases in intact rats, in close contact with several GAD65 positive boutons leading to the formation of clusters composed of 2 or more P-boutons around a single Ia afferent fiber (Fig. 3A1, A2). After S_2-transection, the number of vGLUT1 positive afferents in lamina IX per S_3–S_4 spinal cord cross section did not change significantly in comparison to intact control animals ($P=0.3799$, one-way ANOVA; Fig. 3B1, B2, C). However, the number of P-boutons and the number of P-boutons per afferent fiber was significantly and persistently decreased 1 week following injury ($P=0.0119$ for P-boutons, $P<0.0001$ for P-boutons per vGLUT1 positive afferent fiber, one-way ANOVA; Fig. 3D, E). One week after lesion the number of P-boutons per afferent fiber was substantially reduced by more than 50% (Fig. 3E). 12 weeks after injury the ratio slightly recovered, but remained far below the level of intact animals. Analysis of the composition of the P-bouton clusters showed that the percentage of afferent fibers associated with 2 or more boutons decreased after SCI ($P<0.001$, one-way ANOVA; Fig. 3F–J). These data suggest an early and extensive reduction of the presynaptic GABAergic inhibition of Ia afferent fibers in the ventral spinal gray matter below the injury site.

Based on these findings, we then investigated whether the reduced cholinergic motoneuronal input and the decreased axo-axonal GABAergic innervation in lamina IX after complete SCI were also associated with changes of number and size of cholinergic and GABAergic spinal interneurons. The cholinergic interneurons giving rise to C-boutons are primarily located in lamina VII in close proximity to the central canal (Huang et al., 2000; Miles et al., 2007;

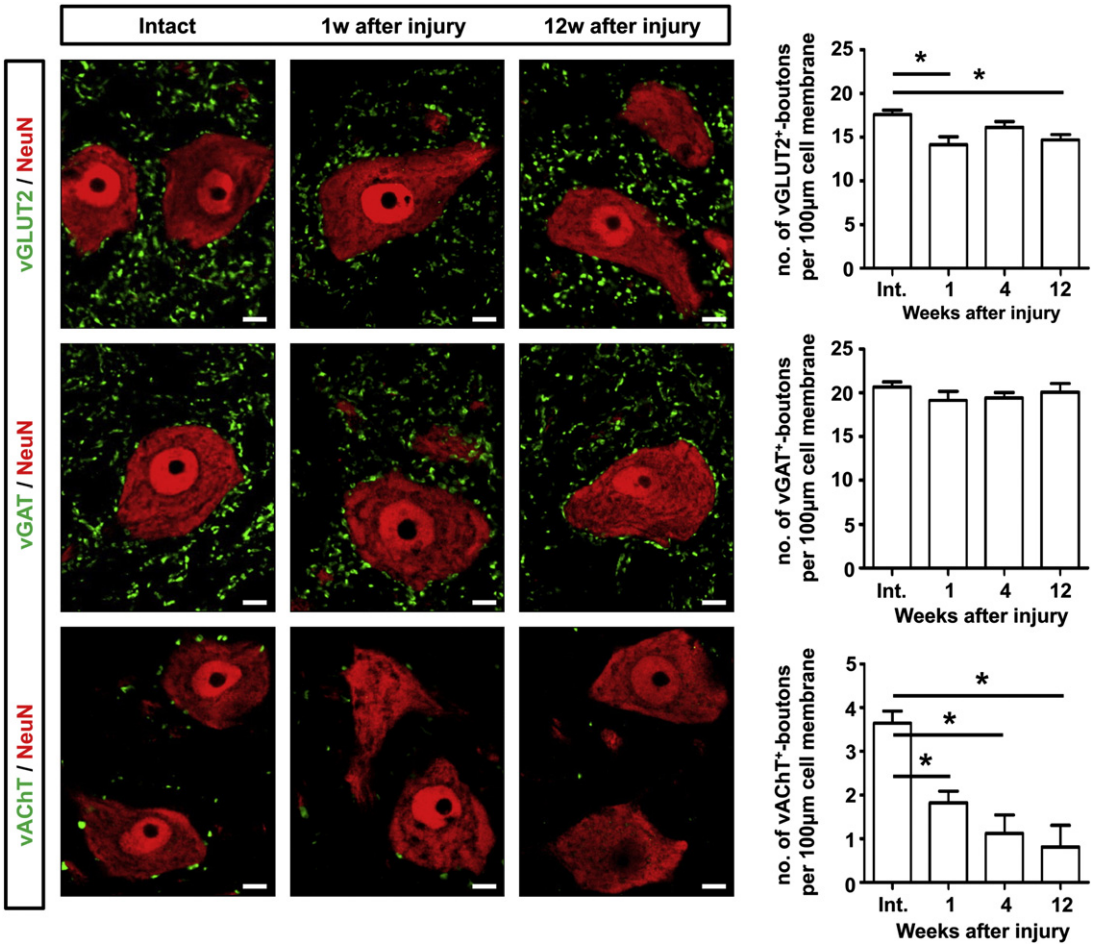

Fig. 2. Quantification of glutamatergic, GABAergic and cholinergic synaptic inputs on motoneuron somata located in segments S_3–S_4 below the lesion site demonstrates a substantial loss of cholinergic C-boutons. The numbers of excitatory (vGLUT2), inhibitory (vGAT) and cholinergic boutons (vAChT) apposed on sacral motoneuron somata (NeuN positive) are expressed per 100 μm neuronal surface membrane for intact rats and rats with SCI at different time points after injury. Data are presented as animal group means ± S.E.M., n = 5–11 animals per group. Int., intact. Scale bars: 10 μm. *$P<0.05$.

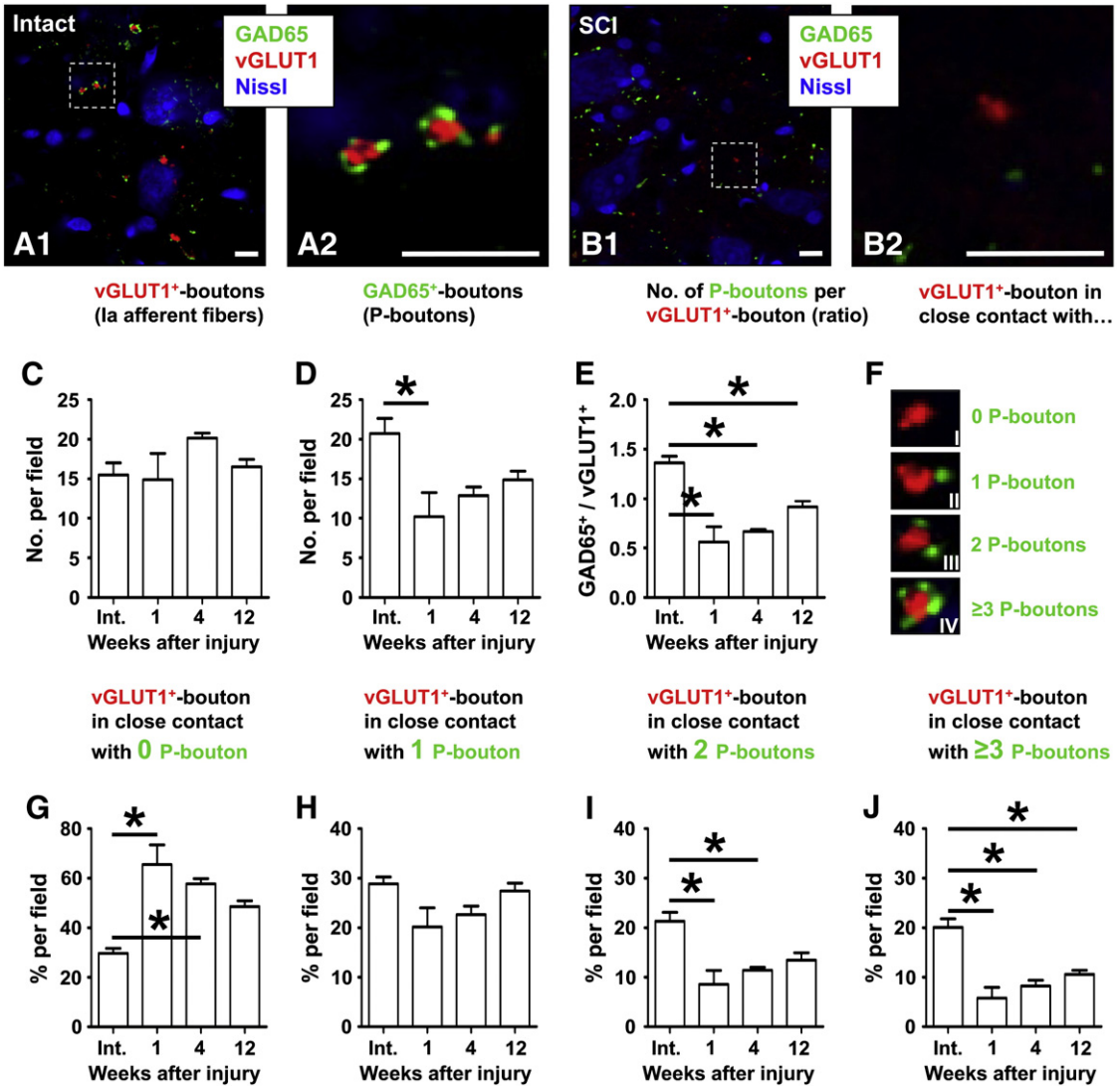

Fig. 3. Quantification of P-boutons in the ventral spinal gray matter (Rexed's lamina IX) below the injury site indicates decreased presynaptic inhibition after complete sacral SCI. (A1, B1) Confocal images of S_3-S_4 ventral spinal gray matter of an intact rat and a rat with sacral SCI. GAD65 positive P-boutons are labeled in green, vGLUT1 positive boutons (Ia afferent fibers) are labeled in red, motoneurons are stained with fluorescent Cresylviolet (blue). A2 and B2 show higher magnification of the areas outlined by the dashed box in A1 and B1, respectively. Scale bars: 10 μm. (C, D) Total numbers of vGLUT1 positive boutons and GAD65 positive P-boutons in the ventral sacral spinal gray matter in intact rats and at different time points after SCI. Numbers are given per field (119 μm × 119 μm). (E) Number of GAD65 positive P-boutons per vGLUT1 positive bouton expressed as ratio (GAD65$^+$ boutons:vGLUT1$^+$ boutons). (F) vGLUT1 positive boutons were assigned to one of four categories: I) no association with any P-bouton, II) close contact with one P-bouton, III) close contact with two P-boutons, and IV) close contact with three or more P-boutons. Examples for each category are presented. (G–J) Percentage of vGLUT1 positive boutons of each category per field (119 μm × 119 μm) in intact rats and rats at different time points after sacral SCI. (C–E, G–J) Data are presented as animal group means ± S.E.M., n = 5–7 animals per group. Int., intact. *P<0.05.

Zagoraiou et al., 2009). In the sacral spinal cord of intact rats, we found some large ChAT positive interneurons in the medial portion of lamina VII (Fig. 4A, B). After S_2-transection, the number of cholinergic interneurons remained unchanged (P = 0.5614, one-way ANOVA; Fig. 4C, G). However, the cell bodies of these interneurons were significantly smaller at 4 and 12 weeks following SCI (P = 0.0001, one-way ANOVA; Fig. 4H). Cell body size was reduced by about 25% at these time points after lesion. In addition, the number of cell bodies smaller than 100 μm², usually not observed in intact animals, increased with time after injury (data not shown). These findings suggest substantial atrophy of cholinergic spinal interneurons around the central canal in response to injury. GABAergic GAD65 positive interneurons were found in both, the medial and lateral portion of lamina VII (Fig. 4D) but also in other regions of the spinal cord gray matter. Starting 1 week after SCI, we found a progressive and significant reduction of the number of detectable GABAergic interneurons in the *medial* portion of lamina VII in spinal segments S_3–S_4 (P<0.0001, one-way ANOVA; Fig. 4E, F, I). The size of the remaining interneurons in this region was significantly decreased by about 30% at 4 weeks after lesion (P = 0.0095, one-way ANOVA; Fig. 4J). However, cell number of GABAergic interneurons in the *lateral* portion of lamina VII was only slightly reduced after SCI while their size was not altered (for number P = 0.0352, for size P = 0.1359, one-way ANOVA; Fig. 4K, L) indicating a rather selective loss and degeneration of GABAergic interneurons in the central region of the spinal cord gray matter below the lesion.

Development of spastic symptoms after SCI has been claimed to be due to aberrant sprouting of excitatory primary afferent fibers in the dorsal horn (Krenz and Weaver, 1998; McCouch et al., 1958). To explore whether there was increased sprouting of such afferent fibers following complete sacral SCI in our rats, we measured the optical density after antibody staining for vGLUT1, vGLUT2,

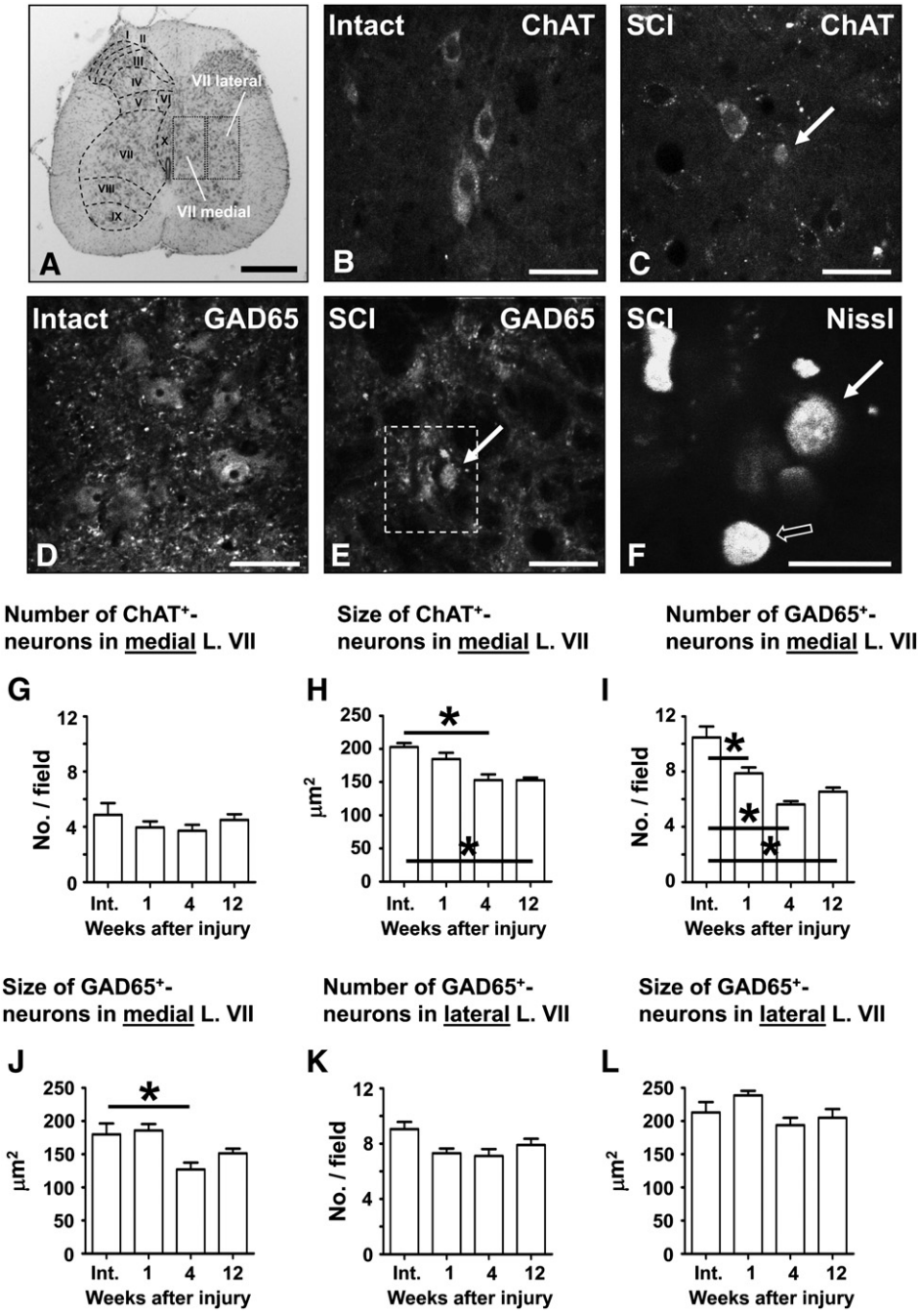

Fig. 4. Reduction of number and size of cholinergic and GABAergic interneurons in the central spinal gray matter (Rexed's lamina VII) below the injury site. (A) Transverse section of the sacral spinal cord stained with Cresylviolet illustrating the areas of analysis (right), i.e. the medial and lateral part of Rexed's lamina VII. Scale bar: 500 µm. (B) Spinal cholinergic interneurons (ChAT positive) in an intact rat. These interneurons can give rise to C-boutons and are exclusively located in the medial part of lamina VII. (C) Spinal cholinergic interneurons in a rat sacrificed 12 weeks after S2-transection. (D) GABAergic sacral interneurons (GAD65 positive) in an intact rat. (E) GABAergic interneurons in a rat sacrificed 12 weeks after SCI. Arrows in C and E indicate small ChAT and GAD65 immunopositive interneurons after SCI, respectively. (B-E): Scale bars: 30 µm. (F) As evidence for a specific GAD65 cell staining, counterstaining with Nissl reveals the presence of GAD65 immunopositive and GAD65 immunonegative cells (black arrow). The solid white arrow points at the same cell as marked in E. The field of view corresponds to the dashed box in E. Scale bar: 15 µm. (G–L) Quantification of number and size of cholinergic (ChAT positive) and GABAergic (GAD65 positive) neurons at different time points after SCI. Results are illustrated for the medial (G–J) and lateral (K–L) part of lamina VII separately. In (G) cell number is given per 10 µm section thickness. (I, K) Number of cells counted per field (224 µm × 224 µm). Data are presented as animal group means ± S.E.M., n = 4–6 animals per group. Int., intact. L, lamina. *$P<0.05$.

GAD65 and vGAT in the superficial laminae I–III of the sacral spinal cord below the lesion site (Table 2). Compared to intact control animals, optical density for vGLUT1 and vGLUT2 showed tendencies to a decrease in injured rats, while the optical density for vGAT was increased and that for GAD65 was decreased. These data do not provide evidence for the presence of massive sprouting of Ia afferent fibers after injury.

Discussion

Two mechanistic models are currently discussed to explain the involuntary spastic muscle contractions that develop over time after a severe spinal cord injury: changes in the electrophysiological properties of motoneurons, and changes in the neuronal connectivity of the spinal segments below the lesion. While a number of recent

experimental studies demonstrated specific changes in NMDA- (N-methyl-d-aspartate), 5-HT- (serotonin), ACh- (acetylcholine) and GABA-receptors as well as ion channels in motoneurons which probably all contribute to hyperexcitability of these cells (Khristy et al., 2009; Li et al., 2004; Murray et al., 2010a, 2010b; Ryge et al., 2010; Wienecke et al., 2010), much less is known about specific changes in excitatory and inhibitory connections to motoneurons and key neuronal premotor circuits. Our immunohistochemical study in rats which developed typical spastic tail cramps and electrophysiological signs of tail spasticity after complete S_2-transection over 1–6 weeks after injury showed a mild decrease of glutamatergic input to motoneuron somata, a fast and massive decrease of cholinergic C-bouton input to motoneuron somata, and a drastic loss of presynaptic GABAergic boutons on Ia primary afferent fibers. The results demonstrate major changes in specific elements of the spinal circuitry, including a decrease of cholinergic excitation to motoneurons and a loss of presynaptic inhibition of Ia fibers and the short-latency stretch reflex pathway.

Loss of all the descending tract synapses including bulbospinal, corticospinal and propriospinal terminals (Masson et al., 1991) in the sacral segments below the S_2-transection resulted in regional 10–50% decreases of glutamatergic vGLUT1 and vGLUT2 positive boutons including the main premotor layer VII at week 1 *post*-lesion. At this time point, only a small decrease of GAD65 positive boutons of less than 10% and no reduction of vGAT positive boutons were observed in lamina VII (and I–III). In contrast, only a minor decrease of glutamatergic boutons of about 20% was seen on somata of sacral spinal cord motoneurons. However, alterations at motoneuron dendrites could not be analyzed by the techniques used. No change was detected in the number of vGAT positive boutons (GABAergic and glycinergic) on motoneuron somata after injury. These results are different from previous data showing an increase of the number of axosomatic glutamatergic boutons after sacral spinal cord injury (Kitzman, 2006). This might be explained by the fact that the overall numbers of glutamatergic and GABAergic boutons observed in this earlier study were much lower than in the present study. It indicates a considerably higher sensitivity of our immunohistochemical technique since a rather large number of boutons on spinal motoneuron somata can be expected based on results from electron microscopic studies (Kullberg et al., 1998; Nacimiento et al., 1995a, 1995b; Ornung et al., 1996).

Two striking observations regarding changes in neuronal connectivity were made. The first change concerns the direct cholinergic input to motoneurons by the C-boutons. These huge excitatory terminals originate from large cholinergic neurons located close to the central canal (Huang et al., 2000; Miles et al., 2007; Zagoraiou et al., 2009). This neuronal system has a key role for motoneuron excitability and function (Zagoraiou et al., 2009). By 1 week after spinal cord transection, the number of C-boutons ending on S_3–S_4 motoneurons dropped to 50%, reaching a low level of 15% at 12 weeks after injury which is comparable to findings by Kitzman (2006). The previously observed up-regulation of genes coding for the nicotinic acetylcholine receptor complex observed in sacral motoneurons after S_2-transection (Wienecke et al., 2010) could well be a compensatory change induced by the loss of cholinergic input. The reduction of cell body diameter of cholinergic neurons in the medial portion of lamina VII at 4–12 weeks after injury is in line with a retraction of their terminals from the motoneurons.

The other striking change concerns the pronounced loss of GABAergic boutons ending presynaptically on Ia fibers in the ventral spinal cord. These P-boutons most likely originate from a specific GABAergic interneuron subpopulation located in the deep medial spinal cord gray matter (Hughes et al., 2005) and are known to mediate powerful presynaptic inhibition of the Ia-mediated (mono- and oligosynaptic) stretch reflex pathways (Betley et al., 2009; Hughes et al., 2005; Nielsen et al., 2007). Our results strongly suggest that facilitation of Ia reflexes, due to the loss of this presynaptic inhibition, represents a key factor for the development of short-latency stretch reflex hyperreflexia and spastic cramps after S_2-transection. A reduced Ia presynaptic inhibition may lead to the increased H-reflex responses typically observed after SCI. An enhanced motoneuron excitability as observed in the rat (present data; (Bennett et al., 1999; Wienecke et al., 2010)), however, has not been seen in humans so far (Dietz, 2010; Faist et al., 1994; Hiersemenzel et al., 2000; Little and Halar, 1985). The shrinkage and loss of GAD65 positive neurons in the medial lamina VII is in line with the pronounced and persistent loss of GABAergic propriospinal connections.

The loss of cholinergic excitatory drive to motoneuron somata may be of importance for the understanding of a second phenomenon observed in the denervated spinal cord below severe injuries: the rapid exhaustion of neuronal activity underlying assisted treadmill locomotion in subjects with chronic SCI (Dietz and Muller, 2004; Muller and Dietz, 2006). Assisted walking in a robotic driven gait orthosis generates afferent input, essentially from load receptors, to the spinal cord leading to activation of the central pattern generator for locomotion and leg muscle EMG activity in paraplegic patients (Dietz, 2010; Dietz et al., 1994, 1995; Rossignol and Frigon, 2011). However, in humans suffering from chronic SCI, the output patterns of extensor and, in particular, flexor motoneurons fade away rapidly, indicating a failure of central excitatory drive (Dietz, 2010; Dietz and Muller, 2004). Given the extensive reduction of cholinergic input on spinal motoneurons after complete S_2-transection (present data, (Kitzman, 2006)) and its putative role for locomotor function in rodents (Zagoraiou et al., 2009), one can speculate that a deficient cholinergic system could be responsible for the rapid exhaustion of leg muscle activity observed in humans with chronic complete SCI. This phenomenon of divergent effects on motoneurons, i.e., hypoexcitation intersecting with hyperactivity for different neuronal motor circuitries, fits with the hyperactivity of short-latency reflexes versus a reduced activity in neuronal circuits underlying locomotion. This aspect is in line with the observation in humans showing exaggerated tendon tap reflexes in clinical spasticity but a reduced muscle activation in spastic movement disorder due to the loss of polysynaptic reflexes (for review see (Dietz and Sinkjaer, 2007)).

The mechanisms underlying the observed atrophy of cholinergic and GABAergic interneurons and the retraction of their propriospinal connections in response to S_2-transection are unknown. Deprivation of supraspinal input could lead to transsynaptic degeneration of specific spinal interneuron subpopulations, e.g., due to withdrawal of trophic support. In the developing cat spinal cord, cholinergic interneurons preferentially emerged in regions which were initially densely innervated by early corticospinal projections (Chakrabarty et al., 2009). Conversely, depriving cholinergic interneurons of corticospinal innervation due to a spinal cord transection could result in degeneration of these interneurons in the adult organism. In a pilot experiment, we injected a retrograde tracer into the lesion site at S_2 immediately after spinal cord transection to label axotomized neurons and to explore the possibility that axotomy of ascending projections of sacral interneurons led to atrophy of interneurons. We found no difference in number and size of labeled spinal interneurons below the injury site in animals sacrificed 1, 4 and 12 weeks *post*-lesion (unpublished data) suggesting the absence of atrophy induced by the axotomy of ascending projections.

In summary, our results show major changes in glutamatergic, GABAergic and cholinergic interneuronal connections to motoneurons and the neuronal circuits interconnected with the Ia pathway below a complete sacral transection. Together with the known alterations of physiological properties of motoneurons, these circuit changes may represent a key element for the development of spastic symptoms in spinal cord injured rats and humans.

Acknowledgments

The authors thank Dr. Michelle Starkey for critically reading the manuscript and Prof. Dr. Wolf Blanckenhorn for help with the

statistics. The present study was supported by grants of the Swiss National Science Foundation (grants 31–63633.00 and 3100AO-122527/1), the National Centre for Competence in Research "Neural Plasticity & Repair" of the Swiss National Science Foundation, the Spinal Cord Consortium of the Christopher and Dana Reeve Foundation and the Framework Program 7 EU Collaborative Project SPINAL CORD REPAIR.

References

Adams, M.M., Hicks, A.L., 2005. Spasticity after spinal cord injury. Spinal Cord 43, 577–586.
Alvarez, F.J., Villalba, R.M., Zerda, R., Schneider, S.P., 2004. Vesicular glutamate transporters in the spinal cord, with special reference to sensory primary afferent synapses. J. Comp. Neurol. 472, 257–280.
Arvidsson, U., Riedl, M., Elde, R., Meister, B., 1997. Vesicular acetylcholine transporter (VAChT) protein: a novel and unique marker for cholinergic neurons in the central and peripheral nervous systems. J. Comp. Neurol. 378, 454–467.
Bennett, D.J., Gorassini, M., Fouad, K., Sanelli, L., Han, Y., Cheng, J., 1999. Spasticity in rats with sacral spinal cord injury. J. Neurotrauma 16, 69–84.
Bennett, D.J., Li, Y., Harvey, P.J., Gorassini, M., 2001. Evidence for plateau potentials in tail motoneurons of awake chronic spinal rats with spasticity. J. Neurophysiol. 86, 1972–1982.
Bennett, D.J., Sanelli, L., Cooke, C.L., Harvey, P.J., Gorassini, M.A., 2004. Spastic long-lasting reflexes in the awake rat after sacral spinal cord injury. J. Neurophysiol. 91, 2247–2258.
Betley, J.N., Wright, C.V., Kawaguchi, Y., Erdelyi, F., Szabo, G., Jessell, T.M., Kaltschmidt, J.A., 2009. Stringent specificity in the construction of a GABAergic presynaptic inhibitory circuit. Cell 139, 161–174.
Chakrabarty, S., Shulman, B., Martin, J.H., 2009. Activity-dependent codevelopment of the corticospinal system and target interneurons in the cervical spinal cord. J. Neurosci. 29, 8816–8827.
Chaudhry, F.A., Reimer, R.J., Bellocchio, E.E., Danbolt, N.C., Osen, K.K., Edwards, R.H., Storm-Mathisen, J., 1998. The vesicular GABA transporter, VGAT, localizes to synaptic vesicles in sets of glycinergic as well as GABAergic neurons. J. Neurosci. 18, 9733–9750.
Courtine, G., Song, B., Roy, R.R., Zhong, H., Herrmann, J.E., Ao, Y., Qi, J., Edgerton, V.R., Sofroniew, M.V., 2008. Recovery of supraspinal control of stepping via indirect propriospinal relay connections after spinal cord injury. Nat. Med. 14, 69–74.
Delwaide, P.J., Penders, C.A., 1969. Experimental studies on the pathophysiology of spasticity. Electroencephalogr. Clin. Neurophysiol. 27, 727.
Dietz, V., 2010. Behavior of spinal neurons deprived of supraspinal input. Nat. Rev. Neurol. 6, 167–174.
Dietz, V., Muller, R., 2004. Degradation of neuronal function following a spinal cord injury: mechanisms and countermeasures. Brain 127, 2221–2231.
Dietz, V., Sinkjaer, T., 2007. Spastic movement disorder: impaired reflex function and altered muscle mechanics. Lancet Neurol. 6, 725–733.
Dietz, V., Colombo, G., Jensen, L., 1994. Locomotor activity in spinal man. Lancet 344, 1260–1263.
Dietz, V., Colombo, G., Jensen, L., Baumgartner, L., 1995. Locomotor capacity of spinal cord in paraplegic patients. Ann. Neurol. 37, 574–582.
Faist, M., Mazevet, D., Dietz, V., Pierrot-Deseilligny, E., 1994. A quantitative assessment of presynaptic inhibition of Ia afferents in spastics. Differences in hemiplegics and paraplegics. Brain 117 (Pt 6), 1449–1455.
Gilmor, M.L., Nash, N.R., Roghani, A., Edwards, R.H., Yi, H., Hersch, S.M., Levey, A.I., 1996. Expression of the putative vesicular acetylcholine transporter in rat brain and localization in cholinergic synaptic vesicles. J. Neurosci. 16, 2179–2190.
Giuffrida, R., Rustioni, A., 1989. Glutamate and aspartate immunoreactivity in corticospinal neurons of rats. J. Comp. Neurol. 288, 154–164.
Gorassini, M.A., Knash, M.E., Harvey, P.J., Bennett, D.J., Yang, J.F., 2004. Role of motoneurons in the generation of muscle spasms after spinal cord injury. Brain 127, 2247–2258.
Helgren, M.E., Goldberger, M.E., 1993. The recovery of postural reflexes and locomotion following low thoracic hemisection in adult cats involves compensation by undamaged primary afferent pathways. Exp. Neurol. 123, 17–34.
Hiersemenzel, L.P., Curt, A., Dietz, V., 2000. From spinal shock to spasticity: neuronal adaptations to a spinal cord injury. Neurology 54, 1574–1582.
Huang, A., Noga, B.R., Carr, P.A., Fedirchuk, B., Jordan, L.M., 2000. Spinal cholinergic neurons activated during locomotion: localization and electrophysiological characterization. J. Neurophysiol. 83, 3537–3547.
Hughes, D.I., Mackie, M., Nagy, G.G., Riddell, J.S., Maxwell, D.J., Szabo, G., Erdelyi, F., Veress, G., Szucs, P., Antal, M., Todd, A.J., 2005. P boutons in lamina IX of the rodent spinal cord express high levels of glutamic acid decarboxylase-65 and originate from cells in deep medial dorsal horn. Proc. Natl. Acad. Sci. U. S. A. 102, 9038–9043.
Khristy, W., Ali, N.J., Bravo, A.B., de Leon, R., Roy, R.R., Zhong, H., London, N.J., Edgerton, V.R., Tillakaratne, N.J., 2009. Changes in GABA(A) receptor subunit gamma 2 in extensor and flexor motoneurons and astrocytes after spinal cord transection and motor training. Brain Res. 1273, 9–17.
Kitzman, P., 2005. Alteration in axial motoneuronal morphology in the spinal cord injured spastic rat. Exp. Neurol. 192, 100–108.
Kitzman, P., 2006. Changes in vesicular glutamate transporter 2, vesicular GABA transporter and vesicular acetylcholine transporter labeling of sacrocaudal motoneurons in the spastic rat. Exp. Neurol. 197, 407–419.
Kitzman, P., 2007. VGLUT1 and GLYT2 labeling of sacrocaudal motoneurons in the spinal cord injured spastic rat. Exp. Neurol. 204, 195–204.
Krassioukov, A.V., Weaver, L.C., 1996. Morphological changes in sympathetic preganglionic neurons after spinal cord injury in rats. Neuroscience 70, 211–225.
Krenz, N.R., Weaver, L.C., 1998. Sprouting of primary afferent fibers after spinal cord transection in the rat. Neuroscience 85, 443–458.
Kullberg, S., Ramirez-Leon, V., Johnson, H., Ulfhake, B., 1998. Decreased axosomatic input to motoneurons and astrogliosis in the spinal cord of aged rats. J. Gerontol. A Biol. Sci. Med. Sci. 53, B369–B379.
Landry, M., Bouali-Benazzouz, R., El Mestikawy, S., Ravassard, P., Nagy, F., 2004. Expression of vesicular glutamate transporters in rat lumbar spinal cord, with a note on dorsal root ganglia. J. Comp. Neurol. 468, 380–394.
Li, Y., Gorassini, M.A., Bennett, D.J., 2004. Role of persistent sodium and calcium currents in motoneuron firing and spasticity in chronic spinal rats. J. Neurophysiol. 91, 767–783.
Little, J.W., Halar, E.M., 1985. H-reflex changes following spinal cord injury. Arch. Phys. Med. Rehabil. 66, 19–22.
Llewellyn-Smith, I.J., Weaver, L.C., 2001. Changes in synaptic inputs to sympathetic preganglionic neurons after spinal cord injury. J. Comp. Neurol. 435, 226–240.
Llewellyn-Smith, I.J., Weaver, L.C., Keast, J.R., 2006. Effects of spinal cord injury on synaptic inputs to sympathetic preganglionic neurons. Prog. Brain Res. 152, 11–26.
Mailis, A., Ashby, P., 1990. Alterations in group Ia projections to motoneurons following spinal lesions in humans. J. Neurophysiol. 64, 637–647.
Masson Jr., R.L., Sparkes, M.L., Ritz, L.A., 1991. Descending projections to the rat sacrocaudal spinal cord. J. Comp. Neurol. 307, 120–130.
Maynard, F.M., Karunas, R.S., Waring III, W.P., 1990. Epidemiology of spasticity following traumatic spinal cord injury. Arch. Phys. Med. Rehabil. 71, 566–569.
McCouch, G.P., Austin, G.M., Liu, C.N., Liu, C.Y., 1958. Sprouting as a cause of spasticity. J. Neurophysiol. 21, 205–216.
McIntire, S.L., Reimer, R.J., Schuske, K., Edwards, R.H., Jorgensen, E.M., 1997. Identification and characterization of the vesicular GABA transporter. Nature 389, 870–876.
Miles, G.B., Hartley, R., Todd, A.J., Brownstone, R.M., 2007. Spinal cholinergic interneurons regulate the excitability of motoneurons during locomotion. Proc. Natl. Acad. Sci. U. S. A. 104, 2448–2453.
Muller, R., Dietz, V., 2006. Neuronal function in chronic spinal cord injury: divergence between locomotor and flexion- and H-reflex activity. Clin. Neurophysiol. 117, 1499–1507.
Murray, M., Goldberger, M.E., 1974. Restitution of function and collateral sprouting in the cat spinal cord: the partially hemisected animal. J. Comp. Neurol. 158, 19–36.
Murray, K.C., Nakae, A., Stephens, M.J., Rank, M., D'Amico, J., Harvey, P.J., Li, X., Harris, R.L., Ballou, E.W., Anelli, R., Heckman, C.J., Mashimo, T., Vavrek, R., Sanelli, L., Gorassini, M.A., Bennett, D.J., Fouad, K., 2010a. Recovery of motoneuron and locomotor function after spinal cord injury depends on constitutive activity in 5-HT2C receptors. Nat. Med. 16, 694–700.
Murray, K.C., Stephens, M.J., Ballou, E.W., Heckman, C.J., Bennett, D.J., 2010b. Motoneuron excitability and muscle spasms are regulated by 5-HT2B and 5-HT2C receptor activity. J. Neurophysiol. 105, 731–748.
Nacimiento, W., Mautes, A., Topper, R., Oestreicher, A.B., Gispen, W.H., Nacimiento, A.C., Noth, J., Kreutzberg, G.W., 1993. B-50 (GAP-43) in the spinal cord caudal to hemisection: indication for lack of intraspinal sprouting in dorsal root axons. J. Neurosci. Res. 35, 603–617.
Nacimiento, W., Sappok, T., Brook, G.A., Toth, L., Oestreicher, A.B., Gispen, W.H., Noth, J., Kreutzberg, G.W., 1995a. B-50 (GAP-43) in the rat spinal cord caudal to hemisection: lack of intraspinal sprouting by dorsal root axons. Neurosci. Lett. 194, 13–16.
Nacimiento, W., Sappok, T., Brook, G.A., Toth, L., Schoen, S.W., Noth, J., Kreutzberg, G.W., 1995b. Structural changes of anterior horn neurons and their synaptic input caudal to a low thoracic spinal cord hemisection in the adult rat: a light and electron microscopic study. Acta Neuropathol. 90, 552–564.
Nielsen, J.B., Crone, C., Hultborn, H., 2007. The spinal pathophysiology of spasticity—from a basic science point of view. Acta Physiol (Oxf.) 189, 171–180.
Oliveira, A.L., Hydling, F., Olsson, E., Shi, T., Edwards, R.H., Fujiyama, F., Kaneko, T., Hokfelt, T., Cullheim, S., Meister, B., 2003. Cellular localization of three vesicular glutamate transporter mRNAs and proteins in rat spinal cord and dorsal root ganglia. Synapse 50, 117–129.
Ornung, G., Shupliakov, O., Linda, H., Ottersen, O.P., Storm-Mathisen, J., Ulfhake, B., Cullheim, S., 1996. Qualitative and quantitative analysis of glycine- and GABA-immunoreactive nerve terminals on motoneuron cell bodies in the cat spinal cord: a postembedding electron microscopic study. J. Comp. Neurol. 365, 413–426.
Raineteau, O., Schwab, M.E., 2001. Plasticity of motor systems after incomplete spinal cord injury. Nat. Rev. Neurosci. 2, 263–273.
Rossignol, S., Frigon, A., 2011. Recovery of locomotion after spinal cord injury: some facts and mechanisms. Annu. Rev. Neurosci. 34, 413–440.
Ryge, J., Winther, O., Wienecke, J., Sandelin, A., Westerdahl, A.C., Hultborn, H., Kiehn, O., 2010. Transcriptional regulation of gene expression clusters in motor neurons following spinal cord injury. BMC Genomics 11, 365.
Schwab, M.E., 2010. How hard is the CNS hardware? Nat. Neurosci. 13, 1444–1446.
Todd, A.J., Sullivan, A.C., 1990. Light microscope study of the coexistence of GABA-like and glycine-like immunoreactivities in the spinal cord of the rat. J. Comp. Neurol. 296, 496–505.
Todd, A.J., Hughes, D.I., Polgar, E., Nagy, G.G., Mackie, M., Ottersen, O.P., Maxwell, D.J., 2003. The expression of vesicular glutamate transporters VGLUT1 and VGLUT2 in neurochemically defined axonal populations in the rat spinal cord with emphasis on the dorsal horn. Eur. J. Neurosci. 17, 13–27.

Usdin, T.B., Eiden, L.E., Bonner, T.I., Erickson, J.D., 1995. Molecular biology of the vesicular ACh transporter. Trends Neurosci. 18, 218–224.
Weaver, L.C., Cassam, A.K., Krassioukov, A.V., Llewellyn-Smith, I.J., 1997. Changes in immunoreactivity for growth associated protein-43 suggest reorganization of synapses on spinal sympathetic neurons after cord transection. Neuroscience 81, 535–551.
Wienecke, J., Westerdahl, A.C., Hultborn, H., Kiehn, O., Ryge, J., 2010. Global gene expression analysis of rodent motor neurons following spinal cord injury associates molecular mechanisms with development of postinjury spasticity. J. Neurophysiol. 103, 761–778.
Zagoraiou, L., Akay, T., Martin, J.F., Brownstone, R.M., Jessell, T.M., Miles, G.B., 2009. A cluster of cholinergic premotor interneurons modulates mouse locomotor activity. Neuron 64, 645–662.
Zorner, B., Schwab, M.E., 2010. Anti-Nogo on the go: from animal models to a clinical trial. Ann. N. Y. Acad. Sci. 1198 (Suppl. 1), E22–E34.